

Noninvasive imaging of focal atherosclerotic lesions using fluorescence molecular tomography

Dolonchampa Maji
Metasebya Solomon
Annie Nguyen
Richard A. Pierce
Pamela K. Woodard
Walter J. Akers
Samuel Achilefu
Joseph P. Culver
Dana R. Abendschein
Monica Shokeen

Noninvasive imaging of focal atherosclerotic lesions using fluorescence molecular tomography

Dolonchampa Maji,^{a,b} Metasebya Solomon,^{a,b}
Annie Nguyen,^c Richard A. Pierce,^c
Pamela K. Woodard,^b Walter J. Akers,^b
Samuel Achilefu,^{a,b} Joseph P. Culver,^{a,b}
Dana R. Abendschein,^c and Monica Shokeen^{b,*}

^aWashington University, Department of Biomedical Engineering, One Brookings Drive, St. Louis, Missouri 63110, United States

^bWashington University School of Medicine, Department of Radiology, 4525 Scott Avenue, St. Louis, Missouri 63110, United States

^cWashington University School of Medicine, Center for Cardiovascular Research, Department of Internal Medicine, 660 S. Euclid Avenue, St. Louis, Missouri 63110, United States

Abstract. Insights into the etiology of stroke and myocardial infarction suggest that rupture of unstable atherosclerotic plaque is the precipitating event. Clinicians lack tools to detect lesion instability early enough to intervene, and are often left to manage patients empirically, or worse, after plaque rupture. Noninvasive imaging of the molecular events signaling prerupture plaque progression has the potential to reduce the morbidity and mortality associated with myocardial infarction and stroke by allowing early intervention. Here, we demonstrate proof-of-principle *in vivo* molecular imaging of C-type natriuretic peptide receptor in focal atherosclerotic lesions in the femoral arteries of New Zealand white rabbits using a custom built fiber-based, fluorescence molecular tomography (FMT) system. Longitudinal imaging showed changes in the fluorescence signal intensity as the plaque progressed in the air-desiccated vessel compared to the uninjured vessel, which was validated by *ex vivo* tissue studies. In summary, we demonstrate the potential of FMT for noninvasive detection of molecular events leading to unstable lesions heralding plaque rupture. © The Authors. Published by SPIE under a Creative Commons Attribution 3.0 Unported License. Distribution or reproduction of this work in whole or in part requires full attribution of the original publication, including its DOI. [DOI: 10.1117/1.JBO.19.11.110501]

Keywords: unstable plaque; fluorescence molecular tomography; natriuretic peptide receptor; near-infrared fluorescence.

Paper 140505LR received Aug. 26, 2014; revised manuscript received Oct. 6, 2014; accepted for publication Oct. 13, 2014; published online Nov. 12, 2014; corrected Nov. 14, 2014.

Carotid artery atherosclerosis is classified as an important cause of stroke. Unstable plaque is characterized by an eccentric neointimal lesion with a lipid core covered by a thinning cap of smooth muscle cells, active angiogenesis, increased matrix metalloproteinase activity, and translocation of monocyte/

macrophages that transform into foam cells. Timely noninvasive imaging that could signal prerupture plaque progression will reduce the morbidity and mortality by allowing early intervention.¹ Although positron emission tomography (PET) and magnetic resonance imaging (MRI) are routinely used for metabolic and morphologic imaging, these modalities are not suited for frequent monitoring or even screening of at-risk patients because of ionizing radiation (PET) and expense (PET, MRI). Transcutaneous Doppler and intravascular ultrasound are insensitive to the subtle molecular changes of critical importance. Fluorescence molecular tomography (FMT) is an emerging optical imaging technology that allows tomographic and quantitative visualization of molecular events *in vivo*.² In this study, a custom built, fiber-based, portable, video-rate FMT system was used for proof-of-principle studies to detect C-type natriuretic peptide receptors (NPR-C) on focal atherosclerotic lesions in the superficial rabbit femoral arteries. The FMT system consisted of a flexible imaging pad (3 cm × 3 cm), containing 12 sources 785 nm 20 kHz, and 830 nm 17-kHz laser diodes as excitation source and reference, respectively.³ The detectors allowed for dynamic concurrent acquisition of frequency encoded fluorescence emission (830 nm; 20 kHz) and transmission reference (830 nm; 17 kHz) signals for the fast generation of ratio-metric data for tomographic reconstruction of the tissue volume. The system could report varying concentrations (1 nM to 1 μM) of indocyanine green at various depths up to 13.5 mm with a depth-dependent spatial resolution on the order of 12 mm.³

We used a model of focal atherosclerotic-like plaques in the femoral arteries (located ~1 to 1.5 cm from skin surface) of New Zealand white rabbits. All animal studies performed were approved by the Washington University Animal Studies Committee. Endothelial denudation of surgically exposed right femoral artery was induced by air desiccation of the luminal surface as described previously.⁴ The uninjured left femoral artery served as the internal control. The animals were maintained on a cholesterol-enriched diet (>200 mg/dL in blood), and over time the air desiccation led to a focal lesion. In this animal model, anatomical coregistration was not used because the location of the lesion was apparent due to the surgical markings and identification by the surgeon at each imaging session. In a clinical setting, coregistration of the FMT probe with the ultrasound (US) probe can be utilized. We chose to monitor the progression of the receptor, NPR-C, which has been shown to undergo changes during atherosclerotic plaque progression and was recently evaluated as a PET imaging marker.⁵ NPR-C is a cell surface protein found on endothelial, vascular smooth muscle, and macrophage cells. Natriuretic peptides (NPs) play an important role in regulating cardiovascular homeostasis. NPR-C (clearance receptor) removes NPs from circulation by receptor mediated endocytosis.⁶ We evaluated a bioconjugate LS668 (Cypate-RSSc[CFGGRIDRIGAC]), consisting of a near infrared (NIR) fluorescent dye cypate conjugated to a targeting peptide, C-type atrial natriuretic peptide, specific for NPR-C [Fig. 1(a)]. NIR fluorescent (700 to 900 nm) imaging agents are desirable for *in vivo* imaging due to enhanced depth penetration of NIR light and low tissue autofluorescence.⁷ Cell studies demonstrated that LS668 (1 μM, 30-min incubation at 37°C, 5% CO₂) was selectively internalized by stably transfected 293T-NPR-C cells [Fig. 1(b)].⁸ Internalization was blocked in the presence of excess (100 μM) C-ANF peptide [Fig. 1(c)], and additionally, LS668 did not internalize into the control 293T-NPR-A cells [Fig. 1(d)], supporting receptor mediated

*Address all correspondence to: Monica Shokeen, E-mail: mshokeen@wustl.edu

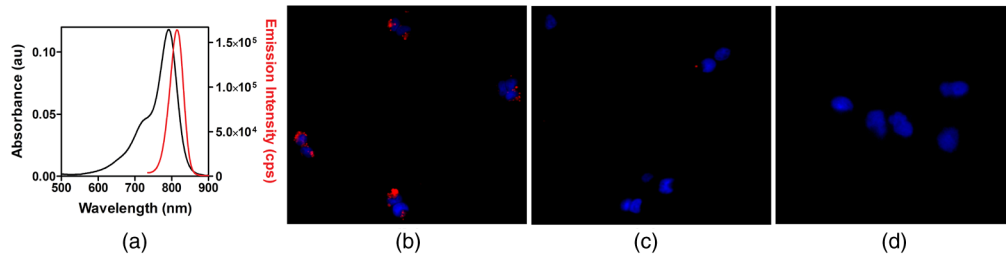


Fig. 1 (a) Absorption and fluorescence spectra of LS668 in dimethylsulfoxide. Fluorescence microscopy images showing cellular internalization of LS668 (b) in NPR-C transfected cells, (c) inhibition of internalization in presence of excess C-ANF peptide, and (d) absence of internalization in NPR-A transfected cells. Blue (DAPI, nuclear stain) and red (LS668). Scale: 100 μm .

endocytosis of LS668. For *in vivo* imaging, 24-h postinjection of LS668 was selected as the optimal time point as clearance of LS668 from blood was achieved at 24 h. Both injured and control femoral arteries of three animals were imaged at day 3 and weeks 1, 2, 4, 6, and 8 following the surgery. For each time point, LS668 (0.1 mg/kg intravenous) was injected and 24 h later FMT scans were performed (5 min each) in triplicates for each artery. FMT reconstruction was performed as reported earlier to obtain three-dimensional (3-D) data from the tissue containing the lesion.³ FMT scans of the respective arteries before surgery were used as blank scans for image reconstruction. In the reconstructed data, localized fluorescence signal indicating accumulation of LS668 was observed at a depth of 4 to 16 mm and over 15 mm of length consistent

with the location of the focal lesion. Coronal section images of the 3-D volumes are shown at a depth of 7 mm for one representative animal [Fig. 2(a)]. The corresponding sagittal and transverse sections show the spread of the lesion along the length and breadth [Figs. 2(a) and 2(b)]. Near background signal from the tissue surrounding the localized fluorescent region indicated negligible nonspecific uptake by surrounding tissue. Contralateral noninjured femoral arteries showed minimal signal indicating negligible background uptake of LS668 in the control artery. Integrated fluorescence signal (directly related to the quantity of LS668 in tissue) was calculated from each tissue volume (thresholded at above 20% of respective maximum signal) [Fig. 2(c)]. Unpaired *t* test (two tailed) showed statistically significant difference between control and injured arteries at week

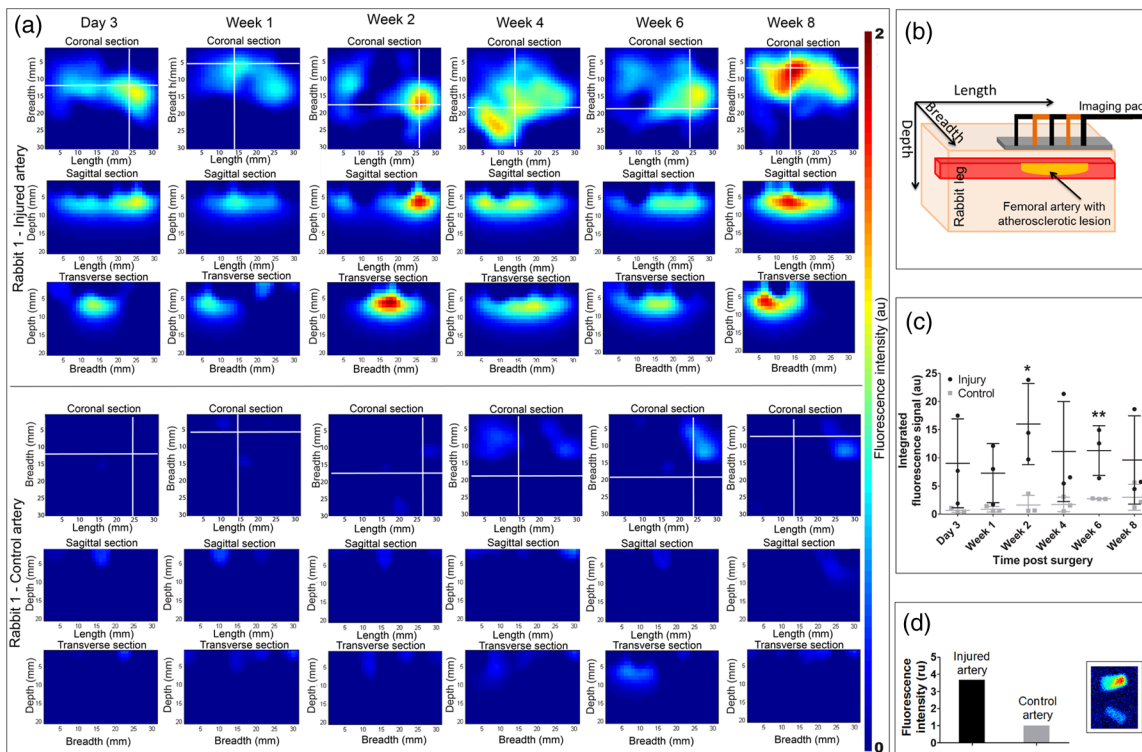


Fig. 2 (a) Coronal (depth = 7 mm), sagittal and transverse sections of reconstructed fluorescence molecular tomography (FMT) signal from injured artery and corresponding control artery from a representative animal (rabbit 1). White lines indicate the position of the respective sagittal and transverse sections. (b) Schematic showing the relationship between the FMT images displayed to their orientation with respect to the tissue volume. (c) Time dependent changes in integrated fluorescence signal (mean \pm SD, $n = 3$) for injured and control arteries ($*P = 0.0283$; $**P = 0.0282$). (d) Mean ($n = 2$) fluorescence intensity obtained from the ex vivo injured artery containing the lesion and the control artery. Adjoining figure (inset) shows the fluorescence images (excitation/emission: 785 nm/ >800 nm) of the injured artery containing the lesion (top) and the control artery (bottom).

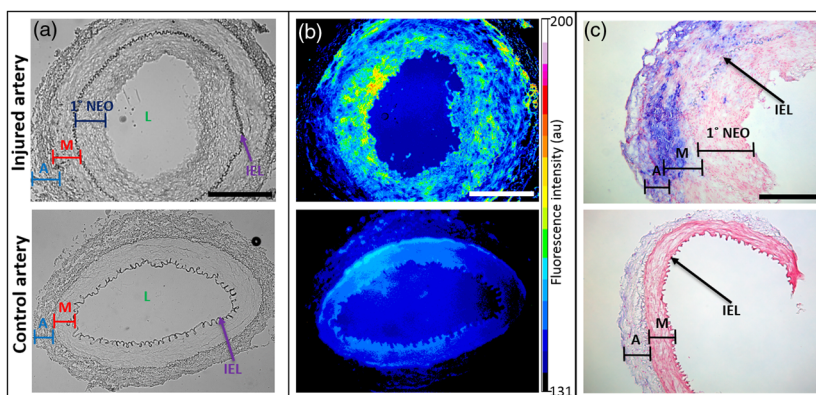


Fig. 3 *Ex vivo* studies on the paraffin fixed sections of injured (top row) and control artery (bottom row) sections obtained at 8 weeks postsurgery. (a) Bright field images showing IEL, internal elastic lamina; A, adventitia; M, media; 1° NEO, primary neointima. Scale: 500 μm . (b) Corresponding fluorescence images (excitation/emission: 710 \pm 75 nm/810 \pm 90 nm) after *ex vivo* staining with LS668. Scale: 500 μm . (c) Immunohistochemistry on tissue sections with clone RAM11 antibody (1: 100 dilution; blue) for macrophages and counterstained with nuclear fast red. Scale: 250 μm .

2 ($P = 0.0283$) and week 6 ($P = 0.0282$) [Fig. 2(c)]. The changes in the signal over time most likely result from a transient increase in macrophages after injury usually at week 2, followed by a decrease resulting from the increased amount of the matrix and decrease in cellularity. Inflammation resumes in the following days or weeks due to the diet-induced macrophage-enriched unstable lesions. The variance within the cohorts highlights the differences in the pace of lesion formation in individual animals, probably as a function of their cholesterol levels. *Ex vivo* tissue biodistribution even after 24-h postinjection at week 8 showed ~ 3.7 -fold ($n = 2$) higher localization of LS668 into the injured femoral artery as compared to the control femoral artery [Fig. 2(d)].

Ex vivo histological validation studies were performed on the arteries at week 8 following the final imaging session. Prior to collecting the arterial segments, the vascular system was flushed with saline and then perfusion fixed with 4% paraformaldehyde and paraffin embedded. Tissue sections were deparaffinized for further studies. The bright-field images of the injured artery showed a thick concentric layer of primary neointima (1° NEO) within the internal elastic lamina (IEL) [Fig. 3(a)]. The control artery showed an intact adventitia (A), media (M), and IEL. *Ex vivo* staining of the injured artery section with LS668 (10 μM ; 30 min; 37°C) followed by fluorescence microscopy showed an increased signal in the layers between A and the lumen (L), which is most likely due to the presence of infiltrating NPR-C expressing macrophages migrating from the adventitia through the media (smooth muscle cells) to accumulate in the base of the NEO closest to the media [Fig. 3(b)]. The control section had a uniform fluorescence signal akin to nonspecific background. Histology sections were also stained for macrophages with mouse monoclonal antibody to rabbit macrophages (clone RAM11). Positive signal was visualized using alkaline phosphatase-conjugated secondary antibody and blue substrate, and nuclear fast red counterstain. In the injured artery, IHC showed a thickened adventitial layer and neointima with a dense accumulation of infiltrating macrophages primarily in the adventitial and medial layers of the injured femoral artery, and also some in the neointima [Fig. 3(c)]. The control artery showed a negligible staining for macrophages. Serial sections were also stained for alpha-smooth muscle actin (SMA). The injured artery demonstrated medial hypertrophy and the staining for alpha-SMA was also markedly higher as compared to the control vessel.

In summary, noninvasive FMT study of atherosclerotic lesions was conveniently performed weekly/biweekly; a feature that is not practical for performing similar PET studies. Sequential imaging with FMT over several weeks showed quantifiable relative changes in the fluorescence intensity that provided insights into receptor concentration as the lesion progressed. This pilot study demonstrates a unique application of an FMT system for serial imaging of focal atherosclerotic plaques in the shallow femoral arteries in a rabbit model of atherosclerosis using a targeted NIR-fluorescent molecular imaging probe. Future studies will incorporate additional NIR-fluorescent imaging agents to serially evaluate the progression of high-risk plaques.

Acknowledgments

We thank S. Grathwohl, P. Baum, K. Liang, G. Sudlow and T. Charanya for their assistance. We also thank the NIH Program of Excellence in Nanotechnology (HL080729), U54CA136398 TSP-1 (S.A.), and U54CA136398 TSP-3 (J.P.C.). D.M. is supported by the NIH 21st Century Imaging Training Grant (T32 EB014855).

References

1. T. Quillard and P. Libby, "Molecular imaging of atherosclerosis for improving diagnostic and therapeutic development," *Circ. Res.* **111**(2), 231–244 (2012).
2. R. Weissleder and V. Ntziachristos, "Shedding light onto live molecular targets," *Nat. Med.* **9**(1), 123–128 (2003).
3. M. Solomon et al., "Video-rate fluorescence diffuse optical tomography for in vivo sentinel lymph node imaging," *Biomed. Opt. Express* **2**(12), 3267–3277 (2011).
4. D. Recchia et al., "The biologic behavior of balloon hyperinflation-induced arterial lesions in hypercholesterolemic pigs depends on the presence of foam cells," *Arterioscler. Thromb. Vasc. Biol.* **15**(7), 924–929 (1995).
5. Y. Liu et al., "Molecular imaging of atherosclerotic plaque with 64Cu-labeled natriuretic peptide and PET," *J. Nuclear Med.* **51**(1), 85–91 (2010).
6. T. Maack, "The broad homeostatic role of natriuretic peptides," *Arq. Bras. Endocrinol. Metabol.* **50**(2), 198–207 (2006).
7. J. V. Frangioni, "In vivo near-infrared fluorescence imaging," *Curr. Opin. Chem. Biol.* **7**(5), 626–634 (2003).
8. D. M. Dickey, D. R. Flora, and L. R. Potter, "Antibody tracking demonstrates cell type-specific and ligand-independent internalization of guanylyl cyclase a and natriuretic peptide receptor C," *Mol. Pharmacol.* **80**(1), 155–162 (2011).